Waypoint navigation for a micro air vehicle using vision-based attitude estimation

J. J. Kehoe, R. S. Causey, M. Abdulrahim and R. Lind
Department of Mechanical and Aerospace Engineering
University of Florida
Florida, USA

ABSTRACT

Missions envisioned for micro air vehicles may require a high degree of autonomy to operate in unknown environments. As such, vision is a critical technology for mission capability. This paper discusses an autopilot that uses vision coupled with GPS and altitude sensors for waypoint navigation. The vision processing analyses a horizon to estimate roll and pitch information. The GPS and altitude sensors then command values to roll and pitch for navigation between waypoints. A flight test of a MAV using this autopilot demonstrates the resulting closed-loop system is able to autonomously reach several waypoints. The vehicle actually uses a telemetry link to a ground station on which all vision processing and related guidance and control is performed. Several issues, such as estimating heading to account for slow updates, are investigated to increase performance.

1.0 INTRODUCTION

A variety of mission scenarios are envisioned for which a micro air vehicle (MAV) would be particularly attractive. A MAV would be ideal to fly around a city looking for biological agents. A MAV would be ideal as a hand-launched platform to provide surveillance over a ridge of a battlefield. A MAV would also be ideal for monitoring and tracking targets in an urban environment. These mission scenarios require the vehicle to operate outside the visual range of a ground operator; consequently, autonomy is a crucial technology for enabling mission capability.

Many organisations around the world have MAV programs which are resulting in a wide range of flying aircraft. Autopilots have even been developed for many vehicles which allow basic autonomy. These autopilots are able to stabilise the vehicle and traverse along a flight path determined by a set of waypoints. The majority of these autopilots have not been documented in archival literature yet; however, several case studies can be found on the internet.

The use of vision is being explored to provide sensing for an autopilot on a MAV. Vision becomes a critical technology when considering mission profiles, such as urban environments, for which a MAV is ideally suited. The existing autopilots almost exclusively rely on gyros and accelerometers along with GPS and altimeters for controlling the vehicle. In actuality, vision may be a primary sensor needed for determining flight path, and potentially even attitude, during highly agile and aggressive maneuvering to explore within a city.

Vision has been used for several control purposes. Many of the studies performed for vision-based vehicle control have involved autonomous ground vehicles using vision sensors for road following[1-6]. Several papers have used similar techniques for flight vehicles such as dirigibles and helicopters[7-9]. The two things the above have in common are 1. they all have the capability to maintain a fixed position for indefinite periods of time to process information, and 2. they all use vision for outer loop tracking purposes. Limited studies make use of vision for control of nonholonomically constrained vehicles such as a fixed wing aircraft[10-13]. Likewise is true for the use of vision for inner loop vehicle stabilisation[10, 12, 14].

This paper discusses a method of waypoint navigation that uses vision-based attitude estimation. A vision system uses an optimal horizon to estimate roll and pitch percentage. Such values note the rotation and vertical displacement of the horizon in the image; consequently, they are not necessarily equal to the standard body-axis measurements of angles but are clearly related. These estimates

Paper No. 3124. Manuscript received 10 August 2006, revised version received 16 October 2006, accepted 7 November 2006.

https://doi.org/10.1017/S000192400000169X Published online by Cambridge University Press



Figure 1. Vision-estimated horizon.

are used by an inner-loop controller for stability and tracking. An outer-loop controller determines a set of roll and pitch commands, which are tracked by the inner-loop controller, to proceed along a pre-determined set of waypoints.

A flight test is performed to demonstrate the methodology and performance of the resulting controller. The MAV is equipped only with a single GPS receiver, an altimeter, and a forward-pointing camera embedded in the nose of the aircraft. As such, the vehicle must rely entirely on the vision system for estimating attitude. The lack of gyros and accelerometers may seem unrealistic and limits the controller to flight in areas where the horizon is obvious; however, the test is indicative of a controller which uses a feature, such as the horizon, for feedback.

The contributions of this paper relate to computing and analysing information associated with vision-based control. In particular, these issues are investigated and detailed in the context of the flight test. One issue is the effect from a roll resolution of ±4·45 deg from the horizon estimation. Another issue is the integration of a 50Hz vision system with a 1Hz GPS system. Also, the issue of using pitch percentage, which is clearly different from pitch angle, is highlighted.

2.0 VISION-BASED ATTITUDE ESTIMATION

2.1 Horizon detection

Evaluation of the horizon is the fundamental technique used in this paper for vision-based attitude estimation. The horizon clearly has limitations due to visibility and ground features; however, the horizon is potentially valuable information. Human pilots often prefer to use visual interpretation of their environment external to the aircraft as a means for stable flight. This paper will build upon an existing technique for horizon detection which was previously used for attitude estimation to stabilise a MAV[12].

The algorithm used for horizon detection uses a statistical measure based on colors. Essentially, statistical modelling is used to classify each pixel by color according to known distribution models which are based on training images. A set of proposed horizons are evaluated to determine which results in the greatest distribution of pixels classified as either ‘ground’ or ‘sky’. The resulting horizon, as shown in Fig. 1, reflects the optimal estimate[12].

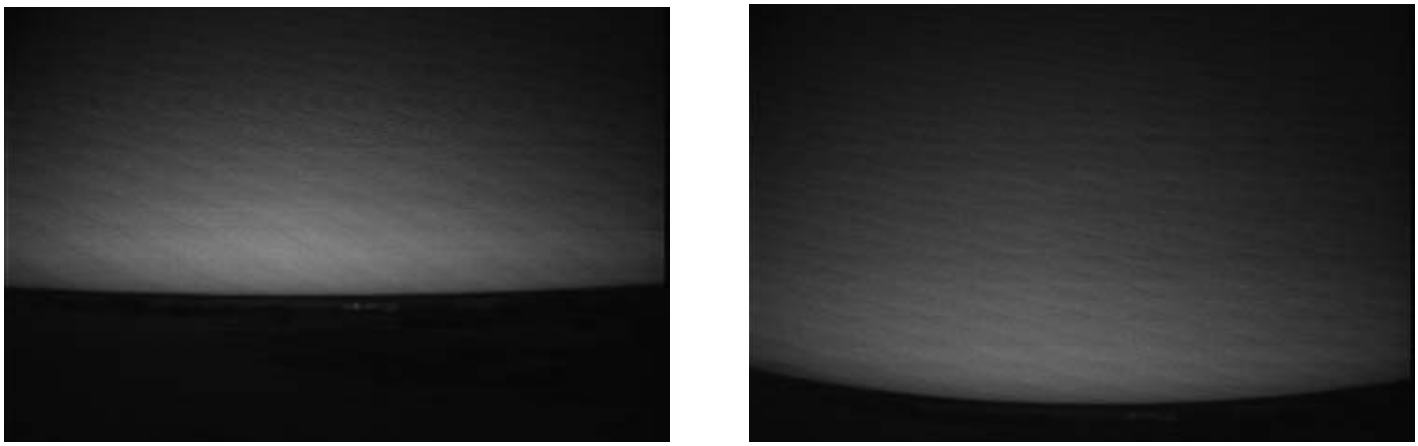
The horizon detection is predicated on several assumptions. The horizon is assumed to appear as a straight line in the image. Also, the horizon is assumed to separate the image into two distinct color groups. Such assumptions obviously limit the usefulness of this approach; however, the horizon detection has been repeatedly shown to be effective in open areas.

2.2 State estimation

Information about the attitude of the aircraft can be inferred based on the horizon in the image coupled with knowledge of the camera relative to the airframe. Clearly a complete set of states can not be estimated based purely on the horizon. In this case, only information related to the roll angle and pitch angle are estimated.

The angular displacement of the horizon can be interpreted as a vision-based estimation of roll angle. This angular displacement should directly correspond to the body-axis roll angle of the aircraft when the pitch angle is negligible. The estimation for non-zero pitch angles will incur some error due to the rotation axis of camera and aircraft. As such, the estimate of roll angle should be considered an estimate whose reliability varies with pitch.

The distribution of sky and ground classification regions is used to determine a parameter denoted pitch percentage. Pitch percentage



(a) (b)

Figure 2. Lens curvature for a horizon.

https://doi.org/10.1017/S000192400000169X Published online by Cambridge University Press

measures the percentage of the image below the vision-estimated horizon and can therefore yield information about the longitudinal attitude of the aircraft. It is important to note this parameter is not concretely tied to any physical coordinate frame. It depends entirely on color and shading in a two-dimensional image. Although a change in pitch attitude will likely result in a change in pitch percentage, a change in pitch percentage does not necessarily indicate a change in pitch attitude. Pitch percentage is also affected by many other factors including altitude, bank and sideslip angles, distance from the physical horizon, and image color abnormalities caused by dark clouds or the sun. Unfortunately, pitch angle can not be uniquely determined because of the many factors affecting pitch percentage; therefore, pitch percentage can not be directly used as an estimate of the pitch angle.

2.3 Issues

The use of computer vision for control purposes presents many advantages; however, it presents many challenges as well. Inherent to the physical system are nonlinearities associated with the camera along with the high risk for interference and noise associated with wireless video transmission[10]. The software poses some issues to address as well due to deviations from the known distribution models in trainer images. Most importantly, vision-based attitude estimation using horizon detection requires that the physical horizon be retained in the image at all times.

A nonlinearity that is inherent to any vision system results from distance. Specifically, the position and size of a feature in the image plane varies inversely with the distance to that feature. This dependence on distance will affect the horizon, and consequently attitude estimation, if the perceived horizon depends on features which are close to the aircraft. Obviously flight amongst trees and mountains will result in features of varying distances and horizons of varying orientation.

Another nonlinearity is associated with lens distortion. The curvature of the lens causes the physical space to be mapped nonlinearly into the image plane in such a way that the image is distorted axisymmetrically. The level of convex and concave distortions increases with distance from the image center, as seen in Fig. 2. At the edge of the image, the mapping of the horizon no longer complies with the straight line assumption of the horizon detection algorithm so some level of error in detection is introduced. This phenomenon has been seen to manifest itself as the horizon 'twitching' as the algorithm jumps back and forth between straight line best guesses along the curved mapping.

Issues are also presented by ambient conditions causing deviations from the trainer images. If color anomalies in the image cause a large enough number of sky or ground pixels to be incorrectly classified, then the distribution split will no longer coincide with the physical horizon. For example, if the algorithm was trained on images of a clear and bright day, then dark clouds introduce sky pixels that do not fit into the known distribution model. These dark pixels may then be erroneously classified as ground pixels and the distribution split no longer lies between the sky and the ground. Other examples of anomalies include bright sunshine associated with sunrise/sunset, dark ground shadows, and sky colors associated with Doppler effect at dusk. Gross misclassification of pixels can cause large erroneous vision-estimated roll angles and pitch percentages.

The most important limitation associated with vision-based attitude estimation using horizon detection is that the horizon must remain in the image at all times. If no sky or equivalently no ground is visible in the image, then some large number of pixels will be misclassified and the estimated horizon will be arbitrary. In this case, the estimated parameters will have no basis in the physical space and any indication of attitude change due to the horizon will be in error. This limitation means that the aircraft must be maneuvered non-aggressively enough that the horizon is always within the camera's field of view.

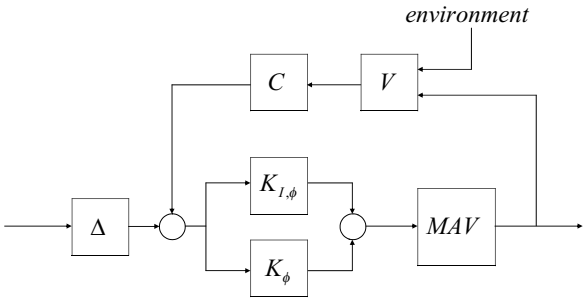


Figure 3. Lateral stability augmentation system.

Finally, interference and noise are inherent to any wireless telemetry system. The interference is often especially prevalent over large distances and for positions near the edge of the receiving antenna's beam width. A large amount of noise distortion in an image will surely have an effect on the color distribution and, therefore, the estimated horizon.

3.0 INNER-LOOP CONTROL

3.1 Lateral stability augmentation system

A stability augmentation system is incorporated into the autopilot to affect the lateral-directional dynamics. Specifically, this system is designed to stabilise the vehicle and provide tracking of roll commands. The architecture for the stability augmentation system is shown in Fig. 3[10].

Tracking performance is achieved using a proportional plus integral controller on an error signal. This error signal derives from subtracting the commanded roll angle from the vision-based roll estimation. The block diagram denotes the vision-based roll estimation resulting the C and V elements. The C element represents the camera whose output is an image resulting from inputs of the aircraft states and the environment. The V element represents the vision processing that computes a roll estimate from extracting a horizon within the image. Also, a low-pass filter is included with the vision processing to reduce anomalies resulting from video transmission or lens distortion.

The actual error signal subtracts a filtered version of the commanded roll angle from the vision-based roll estimate. This filter, represented as Δ, discretises the command to match the vision-based roll resolution of ±4·45 deg. The filter is required to eliminate limit cycles that result from trying to command values of roll angle that can never be measured from the vision system.

The command to differential elevator is finally computed by scaling the filtered error through the controller gains. These gains are denoted as K_ϕ as the proportional gain and KI_ϕ as the integral gain. The integral gain, which is not always included in lateral controllers, is required because asymmetries in construction along with strong torque from the propulsion create a significant steady-state roll moment which must be overcome.

3.2 Longitudinal stability augmentation system

The autopilot also includes a stability augmentation system to affect the longitudinal dynamics. The basic function of this controller is to stabilise the vehicle and track commands to pitch percentage. The resulting architecture is shown in Fig. 4.

This controller acts as a proportional gain on an error signal. The error signal results by subtracting the commanded value of pitch percentage from the vision-based estimate of pitch percentage. The

https://doi.org/10.1017/S000192400000169X Published online by Cambridge University Press

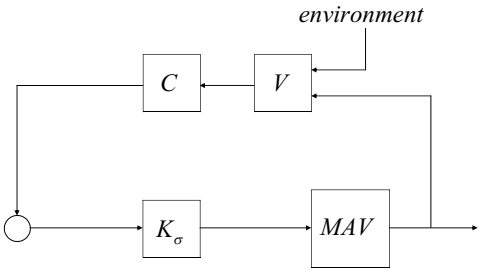


Figure 4. Longitudinal stability augmentation system.

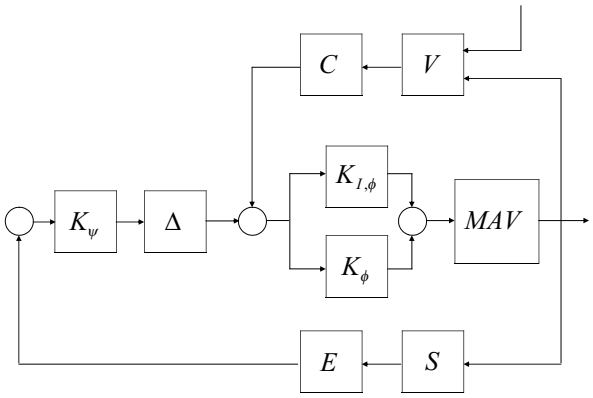


Figure 5. Closed-loop directional control system.

vision-based pitch percentage is estimated from the vision processing, *V*, of the image generated by the camera, *C*, on the aircraft. Finally, the command to symmetric elevator is computed by scaling the error with a proportional gain.

The architecture in Fig. 4 deviates significantly from traditional controllers[16]. Specifically, this controller does not include an integrator which is traditionally included to eliminate steady-state error. The lack of integrator is acceptable because the pitch percentage is not uniquely related to pitch angle. Thus, maintaining straight and level flight does not necessarily require the error in pitch percentage to be negligible or even constant.

The longitudinal controller is designed with questionable value. The controller is useful for situations, such as horizon at infinite distance and airplane at constant altitude, when pitch percentage can be interpreted in terms of pitch. In general, though, the lack of correlation between pitch and pitch percentage reduces the benefit of tracking commands to pitch percentage. This controller will be included as a fall-back element in case of altimeter issues but will be usually be over-ridden by the outer-loop controller for waypoint navigation.

4.0 GUIDANCE AND NAVIGATION

4.1 Heading controller

A heading controller is implemented as an outer-loop lateral-directional compensator. This controller is responsible for steering the vehicle towards the next waypoint throughout a flight. The architecture for the heading controller is presented in Fig. 5.

The closed-loop system in Fig. 5 commands a roll angle to affect heading. Essentially, the error between measured heading and commanded heading is multiplied by a constant gain, K_Ψ, to determine a roll command. This roll command is then limited,

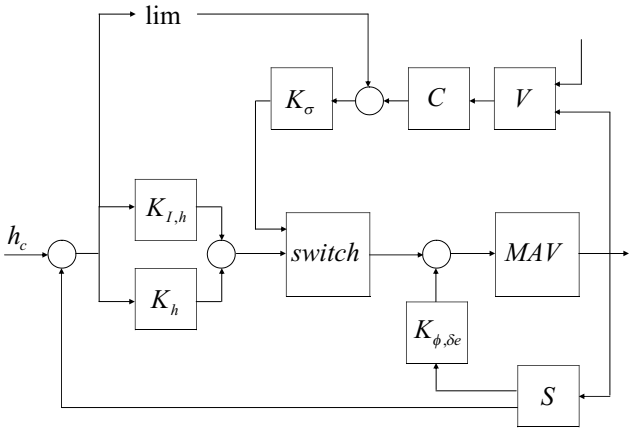


Figure 6. Closed-loop altitude control system.

through the operator noted as Δ in Fig. 5, to ±35·6 deg. This limiting helps to keep the aircraft in a relatively linear fight regime whose flight dynamics are easier to control. Finally, the roll command is used to generate actuation commands through the vision-based roll tracker which is described in Fig. 3.

The compensator also includes an estimator, *E*, to predict the current value of heading. The controller operates at 50Hz; however, the GPS operates at only 1Hz. The aircraft flies at over 10ms^{-1} and can achieve turn rates of 25deg/s so a 1Hz update of heading is clearly insufficient to capture the flight path with high accuracy. Consequently, an estimator is designed to predict the heading at 50 Hz by exploiting an observed proportional relationship between roll angle and heading angle. The heading measurement thus results from combining the GPS and roll angle sensors, given as *S*, at their various rates of update.

4.2 Altitude control

An altitude controller is also included in the autopilot to ensure the MAV reaches the correct altitude associated with each waypoint. This controller commands altitudes of the vehicle throughout the flight path during both straight and turning maneuvers. The architecture for the altitude control is shown in Fig. 6.

The main feature of the altitude controller is the switch element. Essentially, two values of elevator deflection are computed using separate approaches but only one is actually commanded to the servo actuator. The upper path to the switch is simply the inner-loop controller from Fig. 4 that tracks a pitch percentage. The lower path to the switch is a proportional plus integral structure that directly considers an error in altitude.

The upper path is really an augmented version of the tracking controller for pitch percentage in Fig. 4. The augmentation accounts for the need to maintain a visible horizon by including a *lim* block. This block chooses a command to pitch percentage at its maximum limits. The pitch percentage ranges from 0·0 when the horizon is at the bottom of the image to 1·0 when the horizon is at the top of the image. The *lim* block commands a value of 0·2 for a climb or 0·8 for a dive so the vehicle is always commanded to its limit. These limits are chosen so the horizon is never lost. In this way, the controller commands a limiting value of pitch percentage regardless of the actual pitch angle.

The lower path is a standard proportional plus integral controller. The error signal upon which this controller operates is the difference between commanded and measured altitude. Such a controller recognizes the lack of a pitch measurement so, unlike traditional controllers, the altitude error is directly converted to an elevator command[16].

https://doi.org/10.1017/S000192400000169X Published online by Cambridge University Press

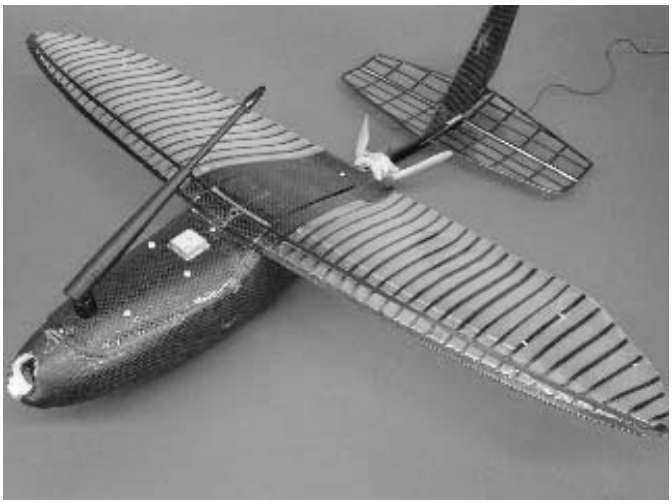


Figure 7. Micro air vehicle.

The switch element chooses the smallest magnitude from the upper and lower paths. Such a choice will minimise the performance of the vehicle in tracking altitude; however, this choice will also minimise the chance of losing visibility of the horizon.

Finally, a gain is included to couple the longitudinal dynamics with the lateral-directional dynamics. This gain, $K_{\phi,\delta}$, generates a command to symmetric elevator based on a measurement of roll angle. The coupling gain is used to improve turn performance by both maintaining altitude and increasing rate of change of heading during a turn.

5.0 FLIGHT DEMONSTRATION

A flight test was performed to demonstrate waypoint navigation using the vision-based attitude estimation. This flight test used the MAV shown in Fig. 7. The vehicle is a variant of MAV which has been designed at the University of Florida[15]. In this case, the MAV is 53cm in length and 61cm in wingspan. The total weight of the vehicle, including all instrumentation, is approximately 540 grams.

The airframe is construScted almost entirely of composite and nylon. The fuselage is constructed from layers of woven carbon fiber which are cured to form a rigid structure. The thin, under-cambered wing consists of a carbon fiber spar-and-batten skeleton that is then covered with a nylon wing skin. A tail empennage, also constructed of composite and nylon, is connected to the fuselage by a carbon-fiber boom that runs concentrically through the pusher-prop disc.

Control is accomplished using a set of control surfaces on the tail. Specifically, a rudder along with a pair of independent elevators can be actuated by commands to separate servos.

The on-board sensors consist of a GPS unit, an altimeter, and a camera. The GPS unit is mounted horizontally on the top of the nose hatch. The altimeter, which uses a measure of pressure, is mounted inside the fuselage under the nose hatch. The video camera is fixed to point directly out the nose of the aircraft. This camera is a pin-hole model with a field of view of 70 deg.

The autopilot operates on an off-board ground station. This ground station essentially consists of a laptop with communication links. Separate streams for video and inertial measurements are sent using transceivers on the aircraft. The image processing and controller analyse these streams and transmit commands to the servos.

Finally, the flight test will occur above a rural area. This area consists of relatively flat and open areas excepting quite a few large trees and some sheds. The aircraft will operate above the tree level and, consequently, should have a clear view of a distant horizon.

Table 1
Controller gains

Gain	Value
K_{ϕ}	0·85
$K_{I,\phi}$	0·04
K_{σ}	–300
K_{h}	–0·25
$K_{I,h}$	–0·006
$K_{\phi,\delta e}$	0·06
K_{ψ}	{0·4, 1·0}

5.1 Controller

The gains for the autopilot were designed based on observing flight properties. Unfortunately, a mathematical model describing the flight dynamics of the MAV did not exist; consequently, a trial and error approach was adopted. A reasonable set of initial gains could actually be derived based on intuition and evaluating aircraft response to human commands. These gains were refined to increase performance both in terms of tracking and navigating.

The final gains are shown in Table 1. These gains correspond to the block diagrams in Figs 5 and 6. The responsive nature of the lateral dynamics allowed for relatively high proportional gain and a fast integrator. Alternatively, the slower nature of altitude response required a limited proportional gain and a relatively slow-acting integrator. Also, several values of K_{Ψ} are presented to reflect the autopilot with and without an estimator for heading angle.

The final gains were based on the ability to continuously attain three pre-programmed waypoints using a relatively smooth flight path. Essentially, the aircraft needed to autonomously reach the waypoints using the smallest possible flight path. The lateral-directional performance was evaluated using a threshold of 0·01 minutes, which corresponds to roughly 5m, around the waypoint for latitude and longitude. The longitudinal performance was not considered critical so the threshold around the waypoint was increased to roughly 12m in altitude. Flight paths that passed within these thresholds were considered to have reached the waypoint so the autopilot then directed the MAV to reach the next waypoint.

5.2 Tracking

The performance of the autopilot for tracking is an important evaluation. The final objective of the autopilot is waypoint navigation; however, this final objective is only reached by the aircraft following commands such as roll and pitch. The ability to quickly follow, and maintain, a required change in roll will obviously affect the ability to reach waypoints so the tracking performance must be investigated.

Figure 8 shows a representative plot of roll response demonstrating the lateral stability augmentation system. Overall, the response tracks reasonably well. Some undesirable dynamic coupling is expected because differential elevator introduces some longitudinal dynamics and because no rudder was used for turn coordination. A short delay time and rise time are exhibited with overshoot on the order of 2-3 bins of resolution (±4·45deg each). Also, oscillations seen between 20-25sec are examples of the horizon ‘twitching’ about two vision-estimated roll angles, which is an issue associated with poor sensor resolution as well as distortions due to lens curvature, which was discussed previously. Good steady-state tracking is seen otherwise.

Figure 9 shows a pitch percentage plot demonstrating the longitudinal stability augmentation system, which uses proportional control to track pitch percentage. Although this controller is used only in specific circumstances as a command limiter, it is important that good general tracking properties are exhibited. The response for this

https://doi.org/10.1017/S000192400000169X Published online by Cambridge University Press

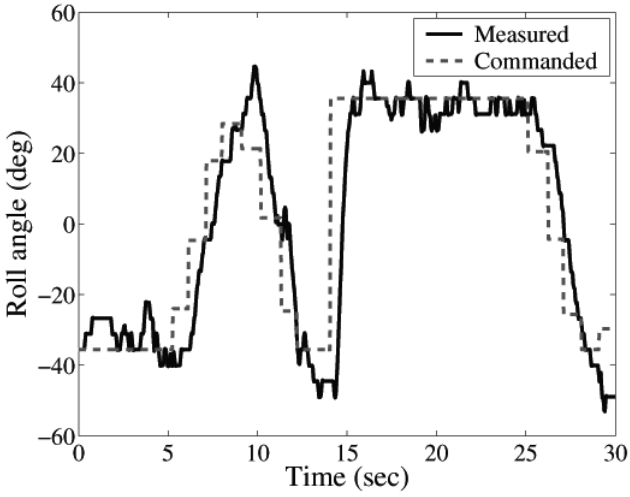


Figure 8. Lateral inner-loop performance.

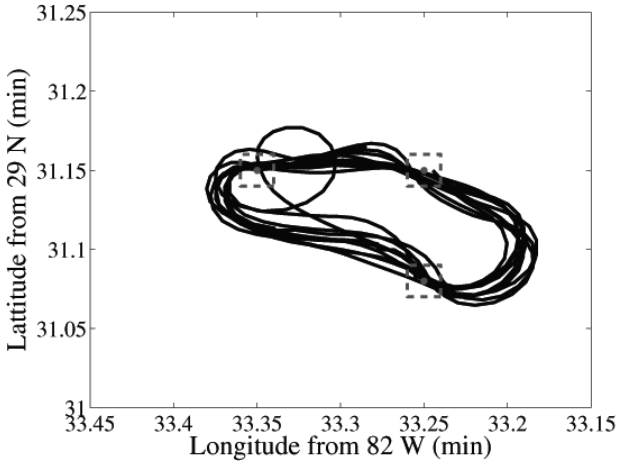


Figure 10. Waypoint navigation with K_ψ = 0·4.

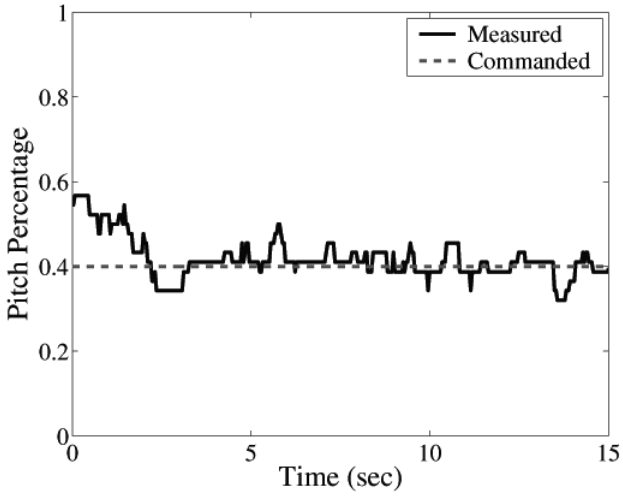


Figure 9. Longitudinal inner-loop performance.

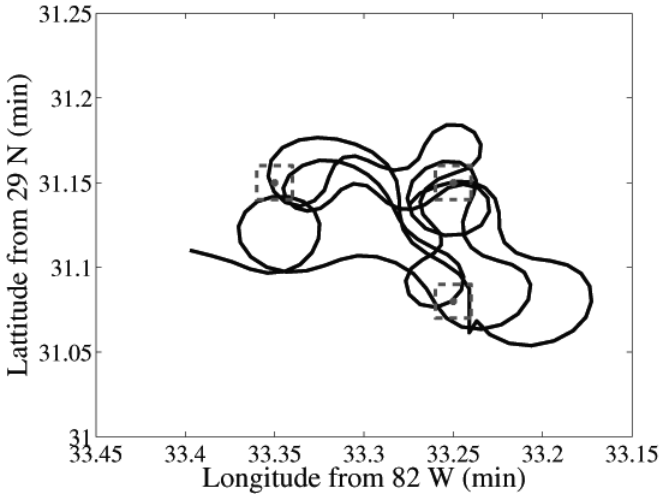


Figure 11. Waypoint navigation with K_ψ = 1·0.

non-aggressive command exhibits reasonably good steady-state tracking. When implemented as a command limiter, some steady-state error can be expected, as the limiting commands correspond to more aggressive attitude changes. These more aggressive values are complemented by associated changes in airspeed which could alter response characteristics undesirably.

5.3 Waypoint navigation

The flight test demonstrated the ability of the autopilot to reach a set of waypoints. In this case, a set of three waypoints were chosen. Each waypoint was separated by distances that could easily be reached by the aircraft within a minute but required some aggressive turns. The altitude of each waypoint was actually chosen to be equal because the climb performance of the vehicle was considerably worse than the turn performance.

The performance of an initial configuration, K_ψ = 0·4 with no heading estimator, is shown in Fig. 10. The plot depicts a GPS map of the waypoint configuration with each of the waypoints shown as a solid dot and the distance threshold the surrounding dashed square. The aircraft clearly attains the waypoints successively; however, the gross acquisition and fine tracking phases of navigation are quite non-aggressive. The acquisition turns are relatively wide and, while the controller is capable of guiding the MAV to within each waypoint threshold, the fine tracking performance does not exhibit enough authority to consistently hit the waypoints with precision. As a result, this autopilot would likely perform poorly and cause excessive circling for waypoints that require aggressive maneuvering.

The autopilot was adjusted to provide more aggressive maneuvering with respect to turns. Specifically, the heading gain was increased such that K_ψ = 1·0 to cause larger turns in response to heading error. The resulting flight path is shown in Fig. 11. The increased gain resulted in sharp turns but also excessive overshoot. As a result, the aircraft frequently missed the waypoint so the flight path displays a non-uniform circling behavior.

The autopilot is challenged by an issue related to time scales; namely, the time scale of the GPS measurements is considerably greater than the time scale of the flight dynamics. Essentially, the MAV can turn and cause considerable changes in flight path much

https://doi.org/10.1017/S000192400000169X Published online by Cambridge University Press

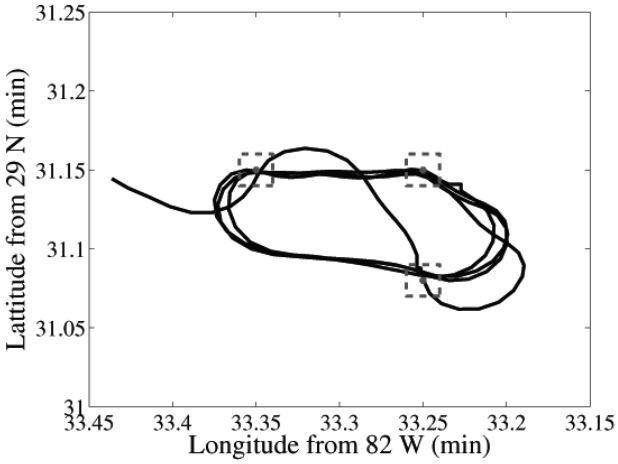


Figure 12. Waypoint navigation with K_{ψ} = 1·0 and heading estimator.

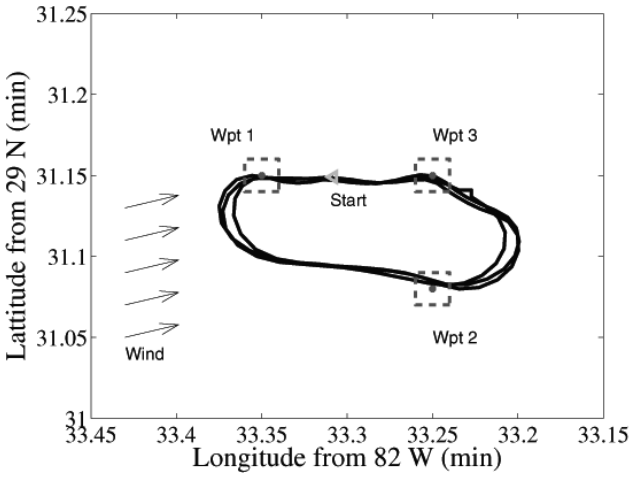


Figure 13. Wind relative to flight path.

faster than then the 1Hz updates from the GPS sensor. As a result, the aggressive controller commanded a fast turn but the nose moved too far before the controller received feedback about the new heading. The flight path in Fig. 11 shows the overshoots that result from a fast rate of turn but a slow rate of heading measurement.

The estimator for heading is incorporated into the autopilot. The resulting flight path is shown in Fig. 12. The estimator is able to predict the heading angle during turns at 50Hz to provide feedback for the autopilot. Consequently, the autopilot can command an aggressive turn for an amount of time suitable to the flight dynamics regardless of the GPS rate.

Clearly the estimator significantly improved performance of the autopilot for waypoint navigation. The large heading changes required during gross acquisition immediately after hitting a waypoint are observably more aggressive in Fig. 12 than in Fig. 10. Conversely, the fine tracking phase of navigation in Fig. 12 exhibits little of the overshoot seen in Fig. 11. A representative flight path through the waypoints was selected for the case shown in Fig. 10 and measured out to 518·8m while a representative track with the estimator running only covered 473·7m of ground.

The estimator also affects several features of the flight data. One effect is the use of estimated data maintains a more uniform flight path from pass to pass. Another effect is the vehicle consistently tracks to within a short distance of the actual target at the center of the waypoint threshold. Thus, using rough estimates at 50Hz is shown to increase both aggressiveness and precision.

6.0 CONTROLLER PERFORMANCE ANALYSIS

The data in Fig. 12 indicate reasonable performance of the closed-loop system for waypoint navigation; however, several issues associated with the flight path must be considered along with simply attaining the waypoints. In particular, the performance with respect to altitude hold and gust rejection need to be investigated. Additional sensor measurements must thus be analysed to fully evaluate the controller.

The wind during the flight testing was recorded at 2·25ms^{-1} from the west-southwest. The effect of this wind, whose direction is shown in Fig. 13, is clearly seen in this representative segment of the flight path. The aircraft, which nominally flies about 13·4ms^{-1}, experiences variation in airspeed about 34% from upwind to downwind conditions. The direction of the wind is such that the MAV is blown into the turn when acquiring waypoint-2 but blown out of the turn when acquiring waypoint-3. Consequently, the MAV is somewhat blown downwind during the flight.

The wind also has a noticeable effect on the roll tracking in addition to the turn radius. Essentially, the autopilot is designed for a single airspeed but the vehicle operates over a wide range of airspeed throughout the flight. The inner-loop controller which provides roll tracking, shown in Fig. 3, is thus required to provide sufficient performance despite this variation in airspeed and associated aircraft dynamics.

Figure 14 demonstrates the effect of wind on the inner-loop roll tracker. The vehicle typically iterates between an 8s turn as it acquires waypoint-2, then an 8s turn as it acquires waypoint-3, then a pair of 1s turns to acquire waypoint-1. The turns starting at approximately {3, 42, 84} s are the turns into the wind and show roll angles exceeding the commanded values including an overshoot. Conversely, the turns starting at approximately {19, 58, 100} s are turns out of the wind and show roll angles smaller than the commanded values. These results are directly caused by the variation in control surface effectiveness from the wind.

The altitude, especially during these turns, is another issue of interest because the vehicle is somewhat underpowered. The altitude tracking is shown in Fig. 15 to be reasonable for straight flight but quite poor for turns. The vehicle consistently loses a great deal of altitude during the turns into the wind but considerably less during the turns out of the wind.

The pitch percentage shown in Fig. 16 indicates, as expected, a dramatic increase during times associated with large roll commands. Such increases are indicative of a large nose-down pitch moment. Differential elevator is a major contributor to this moment when steeply banked because of their location aft of the center of gravity. This coupling effect will be more evident when turning into the wind because of the increased elevator effectiveness associated with the change in airspeed. The loss of altitude is abated to some extent by the gain added through $K_{\phi,\delta e}$; however, the altitude loss was still significant for the turn into the wind.

The dependence of flight performance on wind conditions is further demonstrated in Fig. 17. The turn to acquire waypoint-2 corresponds to headings from 270deg to 90deg whereas the turn to acquire waypoint-3 corresponds to headings from 100deg to 310deg, with the wind originating from about 250deg. Both acquisition turns exhibit loss of altitude, however the loss is clearly greatest during the downwind turn to acquire waypoint-2, resulting in the inverted peak seen in Fig. 17 near 100deg. The vehicle recovers altitude during the two segments flown at approximately constant headings of 90deg and 270deg.

https://doi.org/10.1017/S000192400000169X Published online by Cambridge University Press

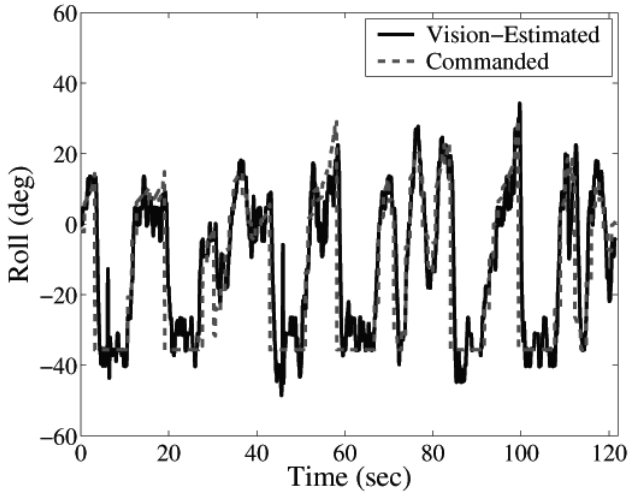


Figure 14. Roll angle.

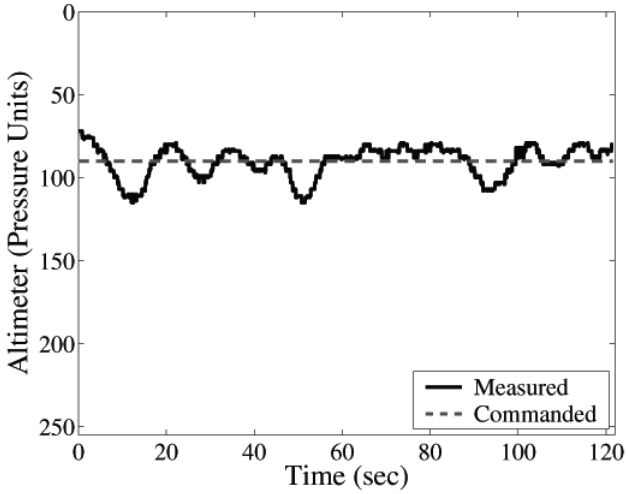


Figure 15. Altimeter.

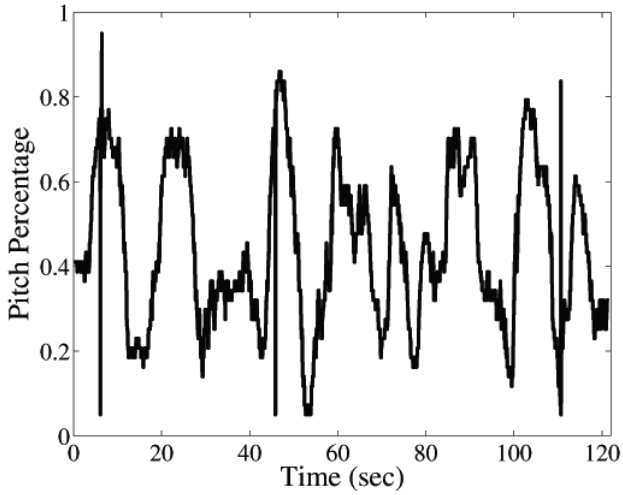


Figure 16. Pitch percentage.

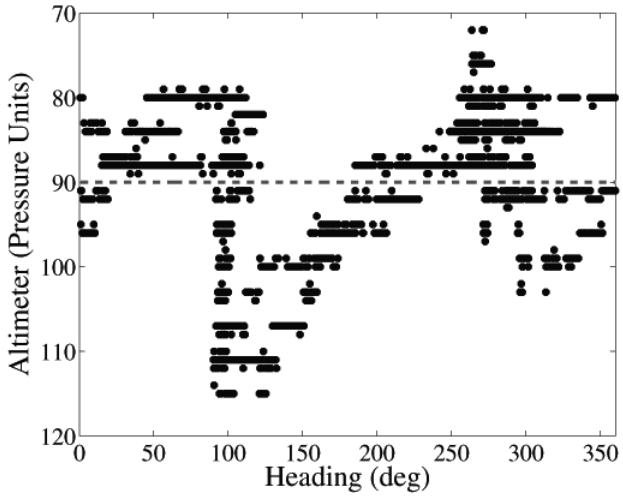


Figure 17. Altimeter relationship to heading.

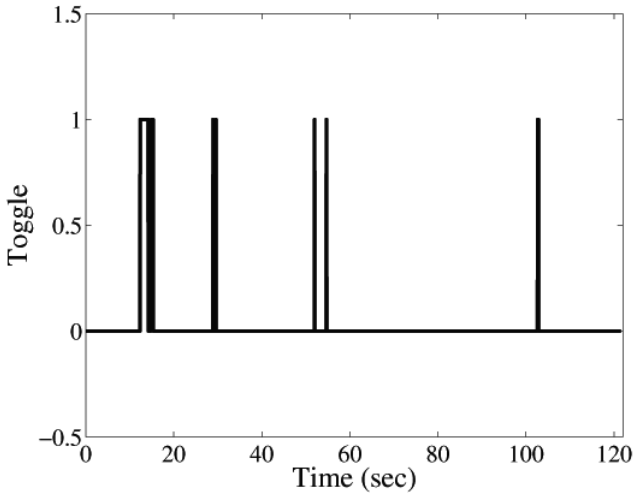


Figure 18. Longitudinal control toggle.

Significant overshoot in climb is seen in theses cases, which is likely due to off-design controller performance resulting from wind effects.

Finally, some discussion is warranted on the function of the switching mechanism in the longitudinal controller shown in Fig. 6. That controller actually has two separate elements that track pitch percentage or track altitude. The switch attempts to retain the horizon in the image, and consequently ensure accurate vision-based attitude estimation, by choosing the less aggressive of the two elements. In this case, the controller will only track pitch percentage when the aircraft has a large error in altitude and the altitude tracker commands an elevator deflection that will pitch the camera image above or below the horizon. The gain, K_σ, is chosen exceedingly large to minimise the magnitude of pitch percentage commands and therefore minimise overshoot while maintaining aggressive tracking near the extreme limits of pitch percentage.

Figure 18 displays instances during the flight test for which the pitch percentage tracking command was used in place of the altitude tracking command. These instances are denoted by values of one in the data set. The controller mostly tracked altitude commands because the flight path rarely required a large pitch which would have lost the horizon. The few instances when the switch activated actually correlate to situations where the error in pitch percentage was coincidentally low so the less aggressive maneuver was to track pitch percentage.

https://doi.org/10.1017/S000192400000169X Published online by Cambridge University Press

7.0 CONCLUSION

This paper has demonstrated that waypoint navigation can be accomplished using GPS and altitude sensing coupled with vision-based attitude estimation. The estimated states are actually only roll angle and pitch percentage; however, these parameters provide sufficient information for basic stability augmentation. A flight test of the resulting autopilot clearly indicates the autopilot performance. In this case, the autopilot is able to generate a short flight path that successively reaches a set of waypoints. The current approach is limited to flight operations in which the horizon is visible; however, the fundamental concept really relates using an autopilot with feedback of a vision-based feature. As such, the autopilot can be extended using this concept to consider other vision-based features, such as building corners or roads, for guidance and navigation.

REFERENCES

1. CASTRO, A.P.A., SILVA J.D. and SIMONI, P.O. Image-based autonomous navigation with fuzzy logic control, 2001, International Joint Conference on Neural Networks, 15-19 July 2001, Volume 3, pp 2200-2205.
2. CHOI, J.Y., KIM, C.S., HONG, S., LEE, M.H., BAE, J.I. and HARASHIMA, F. Vision-based lateral control by yaw rate feedback, 2001, 27th Annual Conference of the IEEE Industrial Electronics Society, 29 November- 3 December 2001, Volume 3, pp 2135-2138.
3. JUBERTS, M. and RAVIV, D. Vision-based vehicle control of AVCS, 1993, Intelligent Vehicles Symposium, 14-16 July 1993, pp 195-200.
4. KOSECKA, J., BLASI, R., TAYLOR C.J. and MALIK, J. A comparative study of vision-based control strategies for autonomous highway driving, 1998, IEEE International Conference on Robotics & Automation, May 1998, pp 1903-1908.
5. MANIGEL, J. and LEONHARD, W. Vehicle control by computer vision, 1992, *IEEE Transactions on Industrial Electronics*, June 1992, **39**, (3), pp 181-188.
6. THOMAS, B.T., LOTUFO, R.A., MORGAN, A.D., MILFORD, D.J. and DAGLESS, E.L. Real-time image analysis for vision-guided vehicle control, 1990, UK IT Conference, 19-22 March 1990, pp 66-70.
7. CAMPOS, M.F.M. and COELHO, L. DE S. Autonomous dirigible navigation using visual tracking and pose estimation, 1999, IEEE International Conference on Robotics and Automation, May 1999.
8. ROCK, S.M., FREW, E.W., HANK, J., LEMASTER, E.A. and WOODLEY, B.R. Combined CDGPS and vision-based control of a small autonomous helicopter, 1998, American Control Conference, June 1998, pp 694-698.
9. SILVEIRA, G.F., CARVALHO, J.R.H., MADIRID, M.K., RIVES, P. and BUENO, S.S. A fast vision-based road following strategy applied to the control of aerial robots, 2001, Brazilian Symposium on Computer Graphics and Image Processing, 15-18 October 2001, pp. 226-231.
10. CAUSEY, R. A Lateral Vision-based Control Autopilot for Micro Air Vehicles using a Horizon Detection Approach, December 2003, MSc Thesis, Department of Mechanical and Aerospace Engineering, University of Florida.
11. CHATTERJI, G.B., MENON, P.K. and SRIDHAR, B. Vision-based position and attitude determination for aircraft night landing, *J Guidance, Control and Dynamics*, January-February 1998, **21**, (1), pp 84-92.
12. ETTINGER, S.M., NECHYBA, M.C., IFJU, P.G. and WASZAK, M.R. Vision-guided flight stability and control for micro air vehicles, 2002, IEEE International Conference on Intelligent Robots and Systems, October 2002.
13. FREW, E., MCGEE, T., KIM, Z., XIAO, X., JACKSON, S., MORIMOTO, M., RATHINAM, S., PADIAL, J. and SENGUPTA, R. Vision-based road-following using a small autonomous aircraft, 2004, IEEE Aerospace Conference, March 2004.
14. KWOLEK, B., KAPUSCINSKI, T. and WYSOCKI, M. Vision-based implementation of feedback control of unicycle robots, 1999, Robot Motion and Control Workshop, 28-29 June 1999, pp 101-106.
15. IFJU, P.G., JENKINS, D.A., ETTINGER, S., LIAN, Y., SHYY, W. and WASZAK, M.R. Flexible-wing-based micro air vehicles, 2002, AIAA 2002-0705.
16. STEVENS, B. and LEWIS, F. *Aircraft Control and Simulation*, 1992, Wiley Inter-Science, New York.

https://doi.org/10.1017/S000192400000169X Published online by Cambridge University Press